ELSEVIER

Journal of Crystal Growth 203 (1999) 570–581

JOURNAL OF CRYSTAL GROWTH

# From $CaSi_2$ to siloxene: epitaxial silicide and sheet polymer films on silicon

Günther Vogg[a,*], Martin S. Brandt[a], Martin Stutzmann[a], Martin Albrecht[b]

[a]*Walter Schottky Institut, Technische Universität München, Am Coulombwall, D-85748 Garching, Germany*
[b]*Institut für Werkstoffwissenschaften, Universität Erlangen-Nürnberg, Cauerstr. 6, D-91058 Erlangen, Germany*

Received 25 February 1999; accepted 9 March 1999
Communicated by K.W. Benz

**Abstract**

The growth of thin epitaxial $CaSi_2$ films with reactive deposition epitaxy (RDE) on different crystalline silicon surfaces is described. The structure and crystalline quality are studied using transmission and scanning electron microscopy as well as X-ray diffraction. Films on (1 1 1)-Si and (1 1 0)-Si in general consist of a mixture of the tr3 and tr6 modifications of $CaSi_2$ and show similar crystalline quality. Epitaxial films of siloxene on (1 1 1)-Si are obtained via topochemical transformation of the corresponding $CaSi_2$ films. X-ray diffraction measurements of siloxene from pure tr6 $CaSi_2$ show that siloxene is also present in a tr6 modification. 

*Keywords:* Calcium disilicide; Siloxene; Reactive deposition epitaxy

## 1. Introduction

Due to their diverse applications and technological importance, silicides are studied intensively [1]. Among the silicides which can be grown epitaxially on Si, the earth alkaline metal disilicide $CaSi_2$ has a unique layered crystal structure (C12-type, [2]) consisting of buckled Si double-layers separated by monolayers of Ca. Earlier studies have shown that $CaSi_2$ exists in two stable trigonal rhombohedral modifications or polytypes (tr3 and tr6), which differ by their stacking sequence [3,4]. Fig. 1 shows the structural details of both modifications. tr6 $CaSi_2$ has a unit cell consisting of six Ca layers, whereas the tr3 unit cell has only three Ca layers. The different stacking sequences are associated with the fact that in the tr6 modification every second Si double-layer is rotated by 180° around the [0 0 .1] direction, whereas in tr3 the Si double-layers are stacked without any rotation.

It is a particular property of $CaSi_2$ that it can be topochemically transformed into a variety of two-dimensional silicon sheet polymers, leaving the Si double-layers intact. The reaction of $CaSi_2$ with concentrated HCl was first performed by Wöhler in 1863 [5], and leads to a material called siloxene or 2D-poly[1,3,5-trihydroxocyclohexasilane] [6]. Siloxene, $Si_6O_3H_6$, as well as the corresponding planar polysilane, $(SiH)_n$ [7], are of basic interest since they are prototypes for two-dimensionally linked silicon structures. Most importantly, these materials are predicted to have an electronic

* Corresponding author. Tel.: + 49-89-289-12768; fax: + 49-89-289-12737.
*E-mail address:* vogg@wsi.tum.de (G. Vogg)

0022-0248/99/$ - see front matter 
PII: S0022-0248(99)00135-9

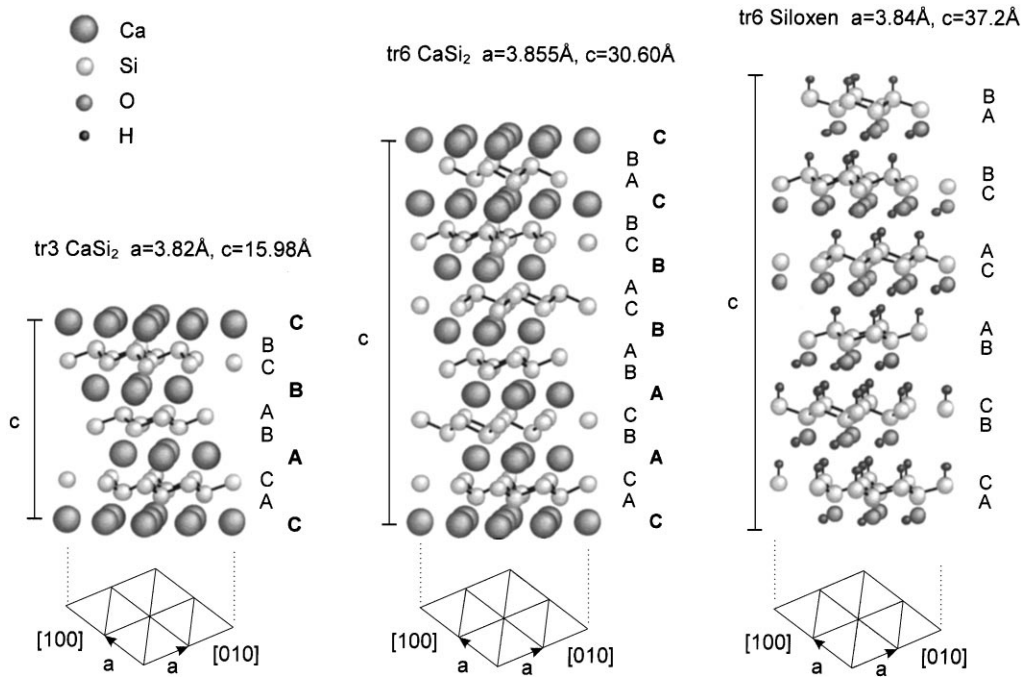


Fig. 1. Crystal structure and lattice constants of the two trigonal rhombohedral modifications tr3 and tr6 of $CaSi_2$ and of the tr6 modification of siloxene.

bandstructure with a direct band gap, which leads to a very efficient visible photoluminescence not exhibited by crystalline silicon.

Siloxene can be prepared in three different forms depending on the starting material $CaSi_2$: microcrystalline powder, single crystal platelets and epitaxial thin layers on silicon substrates. Most of today's knowledge about siloxene originates from studies of powder and single crystal samples. Due to the layered structure of siloxene, most physical properties are expected to be anisotropic. However, the weak bonding between adjacent siloxene layers typically causes large $CaSi_2$ crystals to cleave under chemical transformation, so that only siloxene platelets with a thickness of about 10 μm can be obtained. As will be shown below, epitaxial preparation of siloxene on different silicon surfaces via the method presented here yields highly oriented thin films on large areas which can be used more easily for studies of the material properties than the platelets obtained from $CaSi_2$ crystals. Moreover, the successful realization of electroluminescence of siloxene suggests future device applications like light emitting diodes, for which thin siloxene films are a prerequisite [8]. Since the synthesis via $CaSi_2$ is the only known way to form silicon sheet polymers such as siloxene, it is important for both the investigation of their basic properties as well as for thin film applications to develop a reliable technique for epitaxial growth of $CaSi_2$ on crystalline silicon.

Two approaches have been used to date for the growth of $CaSi_2$ on crystalline silicon: Morar and Wittmer used solid phase epitaxy (SPE) to grow very thin $CaSi_2$ layers by deposition of Ca on room temperature (1 1 1)-Si followed by an anneal [9,10]. In contrast to that, Braungart and Sigmund have exposed a heated Si substrate to Ca vapor and have grown thick $CaSi_2$ platelets on substrates with the same orientation [11]. Using Rutherford backscattering, both groups have shown that only $CaSi_2$ is formed. The fact that none of the Ca-rich phases ($Ca_2Si$ and CaSi) is formed, strongly suggests that Si is diffusing faster in $CaSi_2$ than Ca according to the empirical rules for the diffusion in silicides [12,13]. Additional evidence for this can

be deduced from the film morphology discussed below.

As noted above, the most notable structural feature of $CaSi_2$ and siloxene are the buckled Si double-layers which are also present in crystalline silicon. It is therefore reasonable to assume that templating will take place, i.e. that the (0 0 .1) double-layers in the epitaxial $CaSi_2$ and siloxene layers will be parallel to one of the four {1 1 1}-planes of the crystalline Si substrate. Indeed, Morar et al. have shown that the $CaSi_2$ films can be formed with the buckled layers parallel to the (1 1 1)-surface of silicon, while the platelets grown by Braungart et al. protrude out of the substrate under a certain angle. Fig. 2 shows scanning electron micrographs of $CaSi_2$ grown on differently oriented Si substrates under conditions favoring island growth. The schematic diagrams in the upper part of Fig. 2 represent the orientation of the four {1 1 1}-planes of the cubic Si crystal in relation to the respective substrate. Both Braungart's and Morar's observations can thus be explained with the help of the schematic drawing for (1 1 1)-Si substrates, which shows the three inclined {1 1 1}-Si planes in addition to the (1 1 1)-surface. In case of (1 0 0)-Si substrates, the four equivalent {1 1 1}-planes give rise to a rectangular array of crystallites, which is indeed observed in the respective top view micrograph. For (1 1 0)-Si, two {1 1 1}-planes each are equivalent, which are either exactly perpendicular to or inclined with an angle of about 35° towards the substrate surface. In our study only inclined $CaSi_2$ crystallites were observed on (1 1 0)-Si, so that $CaSi_2$ layer films exhibit a striped morphology. Possible reasons for the observation that $CaSi_2$ does not appear to grow perpendicular to

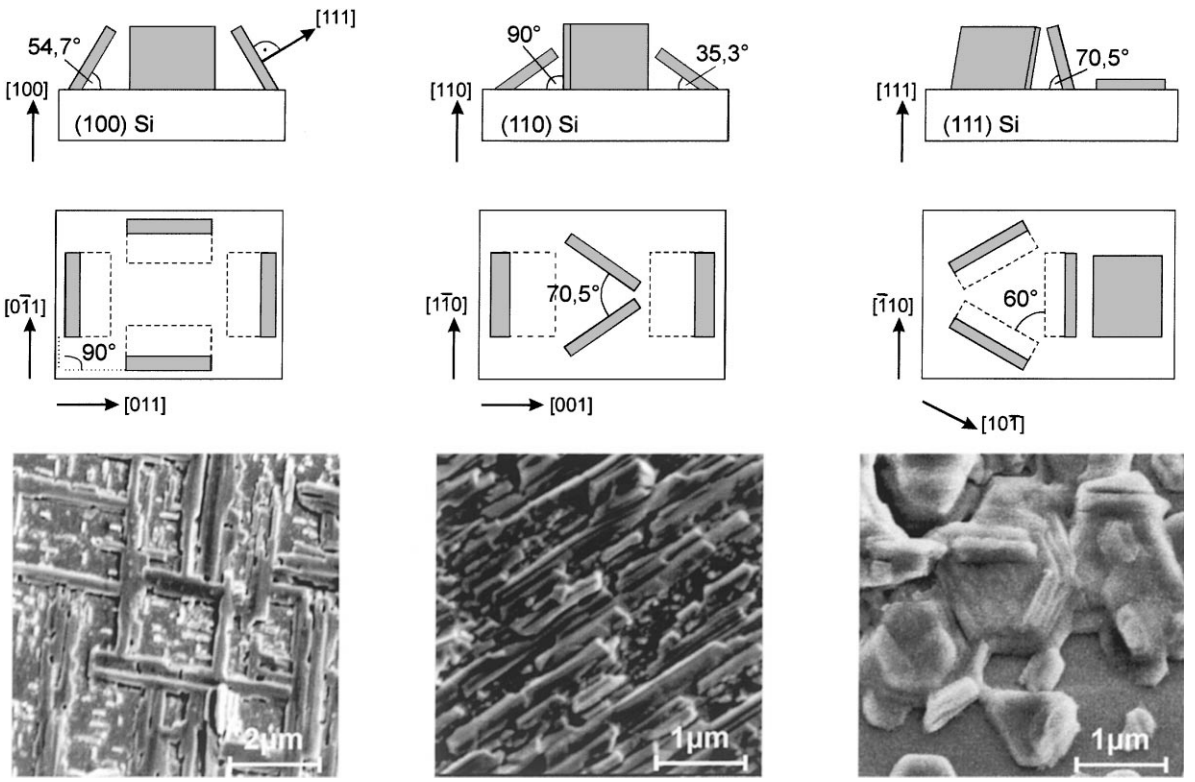


Fig. 2. Comparison of scanning electron micrographs of $CaSi_2$ layers on (1 0 0), (1 1 0) and (1 1 1) crystalline silicon substrates (from left to right, respectively). The upper part shows the schematic side and top views of these substrates with the gray platelets indicating the four independent {1 1 1}-planes of the cubic Si crystal which can act as templates for the $CaSi_2$ growth.

(1 1 0)-Si surfaces will be discussed below. However, the orientation of the substrate can be determined by a simple microscopic inspection of the $CaSi_2$ layer grown on it.

Here, we present a detailed study into the heteroepitaxial growth of $CaSi_2$ on both (1 1 1) and (1 1 0)-Si substrates with reactive deposition epitaxy (RDE), which allows the formation of $CaSi_2$ and siloxene films with layers parallel or inclined with respect to the substrate surface. Using this method we achieve growth of dense $CaSi_2$ films with rocking curve linewidths as low as 0.25°. From these $CaSi_2$ films, epitaxial siloxene can be obtained with a crystalline quality which allows the study of the exact stacking sequence in this material.

## 2. Experimental procedure

Thin epitaxial $CaSi_2$ films were prepared by thermal deposition of pure Ca metal (Aldrich, purity $> 99.5\%$) onto heated silicon substrates with (1 1 1) orientation (on axis) and (1 1 0) orientation (misorientation $< 0.4°$). The substrates were treated with hydrofluoric acid prior to the deposition to remove the native oxide and introduced into the evaporation system under argon atmosphere. The silicon temperature during reactive deposition epitaxy ranged between 700 and 900°C. The growth process leads to a final layer thickness between 100 nm and several μm. To study the different layer morphologies and especially the effect of changing growth conditions on them, the $CaSi_2$ films were examined by scanning electron microscopy (SEM, Hitachi S-3200N) and transmission electron microscopy (TEM, Philips CM 300UT, 300 kV, point resolution 1.7 Å). High resolution X-ray diffraction (HRXRD) measurements were performed on the silicide layers using a Philips Xpert triple axis diffractometer (Cu $K_\alpha$ line, Ge Bartels monochromator and channel-cut Ge analyzing crystal, max. resolution $< 1'$). Some films on (1 1 1)-Si were then transformed into siloxene using Wöhler's method [5]: samples of 0.5 $cm^2$ were covered with 5 ml 37% HCl at 0°C for 30 min, rinsed with water and blown dry. The entire chemical processing was performed under argon atmosphere in a glove box. The resulting siloxene films were examined by XRD under ambient conditions immediately following the chemical transformation.

## 3. Results and discussion

### 3.1. $CaSi_2$ on (1 1 1)-Si

For a small Ca flow, the conditions of reactive deposition epitaxy can be optimized so that thick epitaxial $CaSi_2$ films with Si layers parallel to the substrate surface can be grown [14]. However, island growth still appears to be the dominant growth mechanism, in which hexagonal crystallites formed in the initial growth stage as seen in Fig. 2 later coalesce. Fig. 3a is a SEM top view of such a continuous film and shows the smoothness of the silicide surface which can be obtained. The microcrack was probably caused by thermal strain during the cool down process since the thermal expansion of $CaSi_2$ is remarkably higher than that of Si. In Fig. 3b, a cross-sectional TEM micrograph

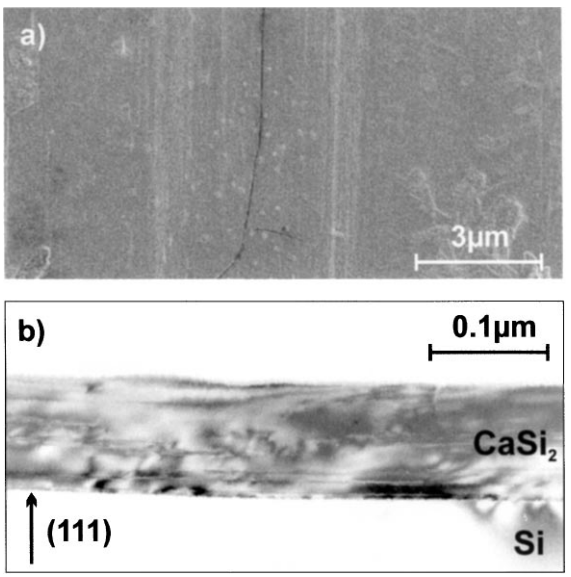


Fig. 3. Top view scanning electron micrograph (a) and cross-sectional transmission electron micrograph (b) of epitaxial $CaSi_2$ on (1 1 1)-Si substrates (substrate temperature $\approx 850$°C, Ca flow $\approx 0.2$ μm/min, growth time 30 min).

of the $CaSi_2$/Si heterostructure is shown. Using HRTEM, the RDE-grown interface can be shown to be atomically abrupt and step-free over extended regions as observed earlier for SPE-grown epilayers [9,10]. Furthermore, Fig. 3b shows that stacking faults parallel to the interface are the dominant structural defects.

When $CaSi_2$ films with a thickness greater than 1 μm are grown, significant substrate erosion takes place, which can lead to a lift-off of parts of or the entire $CaSi_2$ film. This substrate erosion in RDE is due to fact that Si is the faster diffusing species in $CaSi_2$. Therefore, the growth zone is at the Ca/$CaSi_2$ and not at the $CaSi_2$/Si interface. However, we regularly obtain high quality interfaces and films for thicknesses less than 1 μm. It appears that the vacancies caused by the outdiffusion of Si from the substrate can be compensated before they cluster into macroscopic holes. For thicker layers these holes not only decrease the interface quality but also influence the film growth because of laterally inhomogeneous Si diffusion.

We expect the buckled Si double-layers present in both substrate and silicide to determine the relation of epitaxy for $CaSi_2$ on (1 1 1)-Si. Using the hexagonal notation for the tr6 unit cell of $CaSi_2$, the expected relation of epitaxy is given by $(0\,0\,.1)_{CaSi_2} \| (1\,1\,1)_{Si}$ and $[1\,1\,.0]_{CaSi_2} \| [\bar{1}\,1\,0]_{Si}$. Our HRXRD measurements show that the (0 0 .1) plane of the $CaSi_2$ film is indeed parallel to the (1 1 1) plane of the substrate with an accuracy better than 0.02°, consistent with HRTEM. To study the in-plane orientation we have taken pole-figures of the asymmetric $CaSi_2$ *10.7* and the silicon *311* reflexes shown in Fig. 4. The three Si peaks show the three-fold rotation axis of the buckled layer relative to the [1 1 1] direction. Since the three intense $CaSi_2$ diffraction peaks shown in the lower part of Fig. 4 appear at the same positions, the in-plane orientation given above is indeed realized. The additional three weaker diffraction peaks, which are shifted by 60° with respect to the more intense peaks, can be explained by the special structure of the tr6 modification of $CaSi_2$ in which every second Si layer is rotated by 180° around the layer normal. Therefore, a stacking fault is enough for rotating the crystal areas above the fault by 180° relative to the areas below, which would lead to the observed pole-figure. In principle, such a fault could already occur at the $CaSi_2$/Si-interface, resulting in different orientations of adjacent grains. However, the resulting grain boundaries are not observed with TEM.

As mentioned above, $CaSi_2$ exists in the two modifications tr3 and tr6, whose occurrence appears to be influenced by the incorporation of

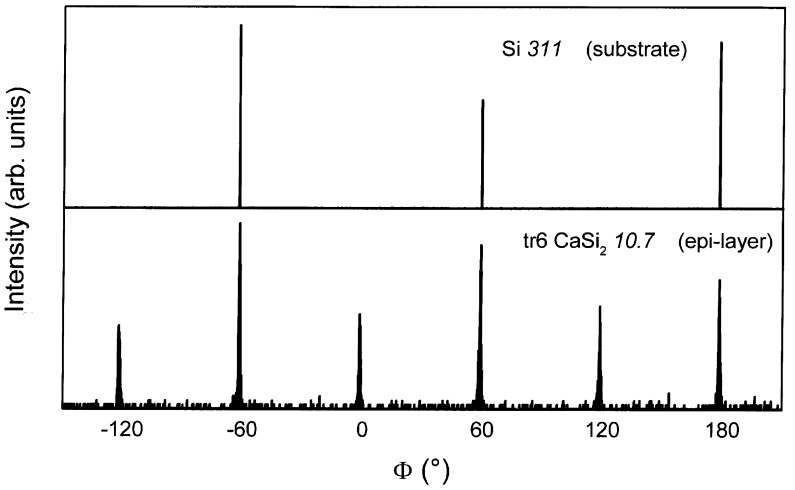


Fig. 4. Pole-figures of the *311* diffraction peak of the (1 1 1)-Si substrate and the *10.7* diffraction peak of the tr6 $CaSi_2$ epilayer. The detector slit width was 0.5°.

impurities. However, it is controversially discussed which modification should be the intrinsic one. Whereas Evers only reports the tr6 modification [3], Janzon and Schäfer find that pure $CaSi_2$ has the tr3 structure and were able to prepare tr6 $CaSi_2$ only after a well defined addition of Sr [4]. Commercial bulk $CaSi_2$ contains a mixture of both modifications. In our RDE-grown $CaSi_2$ films, we generally find both the tr6 and tr3 modifications as well. Fig. 5a shows the symmetric *00.6* and *00.12* diffraction peaks of the tr3 and tr6 modification, respectively, for different total film thicknesses

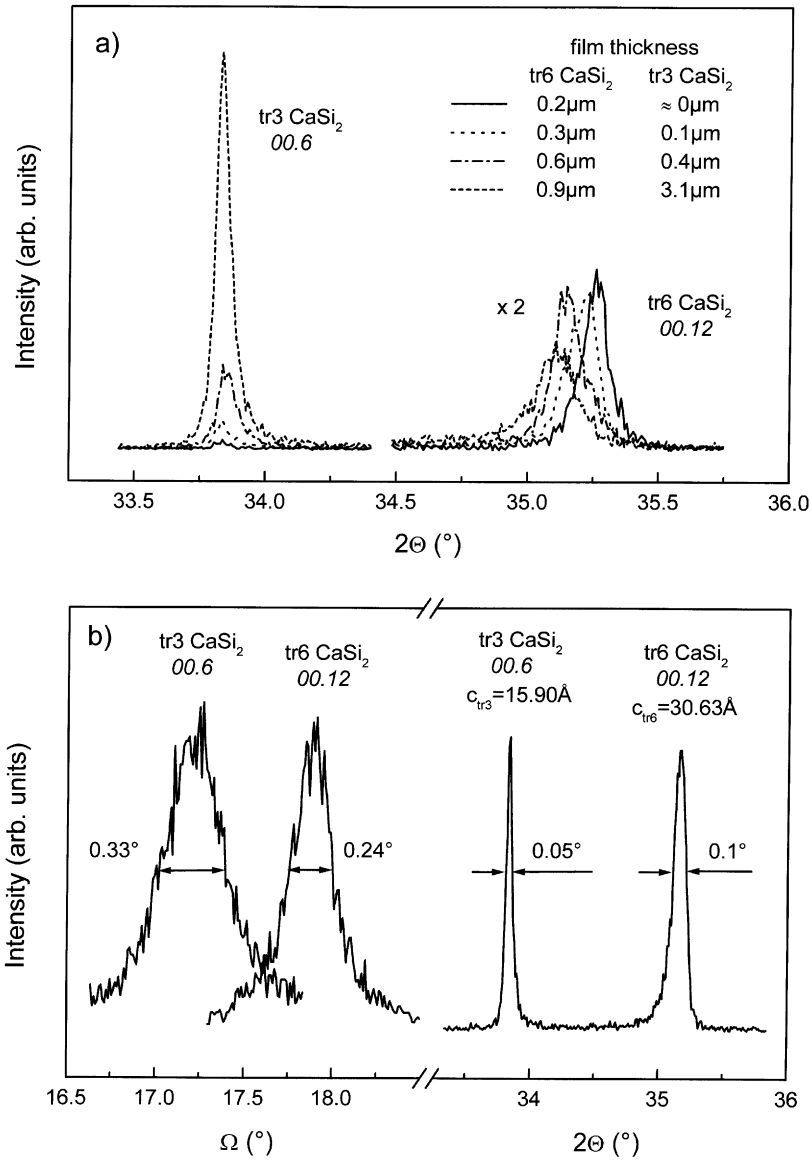


Fig. 5. (a) Bragg–Brentano diffractograms of epitaxial $CaSi_2$ on (1 1 1)-Si with different $CaSi_2$ film thickness (resolution $<1'$). The thickness of the constituent modifications has been estimated as described in the text. (b) Comparison of the Bragg–Brentano and rocking curve line widths of the two modifications present in a 1 µm thick $CaSi_2$ epilayer on (1 1 1)-Si.

measured in Bragg–Brentano geometry. The thickness of the tr3 and tr6 modifications has been estimated from the relative areas under the diffraction peaks and the total layer thickness as determined with SEM. It is obvious that in very thin films only the tr6 modification is present, as already observed by Morar et al. [9,10]. With increasing film thickness, we observe a strong increase of the tr3 contribution. We are therefore led to assume that the tr6 modification is the polytype formed initially and that with increasing film thickness the tr3 polytype is more likely to grow. This could be caused by an increase in the density of stacking faults in thicker films or a reduction of the influence of the Si substrate. Fig. 5b shows a comparison of the typical Bragg–Brentano diffractograms ($2\Theta$) of the symmetric *00.6* and *00.12* reflexes of the tr3 and tr6 modifications and the corresponding rocking curves ($\Omega$) for a $CaSi_2$ film on (1 1 1)-Si with a total thickness of about 1 μm. The broadening of the $2\Theta$ curves with a line width of about 0.1° compared to those of commercial bulk $CaSi_2$ (typically 0.01°) is mainly due to strain between film and substrate. The tr3 modification has a lower $2\Theta$ and a higher $\Omega$ linewidth compared to the tr6 modification because it is less strained but more distorted due to the intermediate tr6 film.

Returning to Fig. 5a, we see that an increasing $CaSi_2$ film thickness results in a shift of the tr6 diffraction peak to lower angles. The corresponding change of the lattice constant $c_{tr6}$ is plotted in Fig. 6 as a function of the tr6 film thickness, together with the corresponding value of $a_{tr6}$ determined from the asymmetric *10.19* reflex. For films with a thickness above 1 μm, $a_{tr6}$ and $c_{tr6}$ are similar to the bulk values. Below 1 μm, one observes a significant dependence of the lattice constant on the film thickness: with decreasing film thickness, $a_{tr6}$ increases and $c_{tr6}$ decreases. This cannot be due to simple mismatch strain caused by the different in-plane lattice constants of Si (3.84 Å) and $CaSi_2$ (3.855 Å), which on the contrary should lead to a decrease of $a_{tr6}$ for very thin films. Since the linear thermal expansion coefficient of $CaSi_2$ ($\Delta a/a \approx 8\times10^{-6}\,K^{-1}$) [15] is higher than that of Si ($\Delta a/a \approx 3\times10^{-6}\,K^{-1}$) no sign reversal of the lattice mismatch takes place at the elevated growth temperatures which could otherwise cause the anomalous shift. However, the films studied here are significantly thicker than the critical layer thickness, which for $CaSi_2$/Si is about 50 nm. Therefore, the films are not grown pseudomorphically but partly or even fully relaxed. Due to the difference in the linear thermal expansion coefficients of $CaSi_2$ and Si the cooling process leads to a temperature induced tensile strain of the originally relaxed film because the Si substrate prohibits the $CaSi_2$ to fully contract which leads to an increased $a_{tr6}$ and a decreased $c_{tr6}$ compared to the room temperature bulk values as observed.

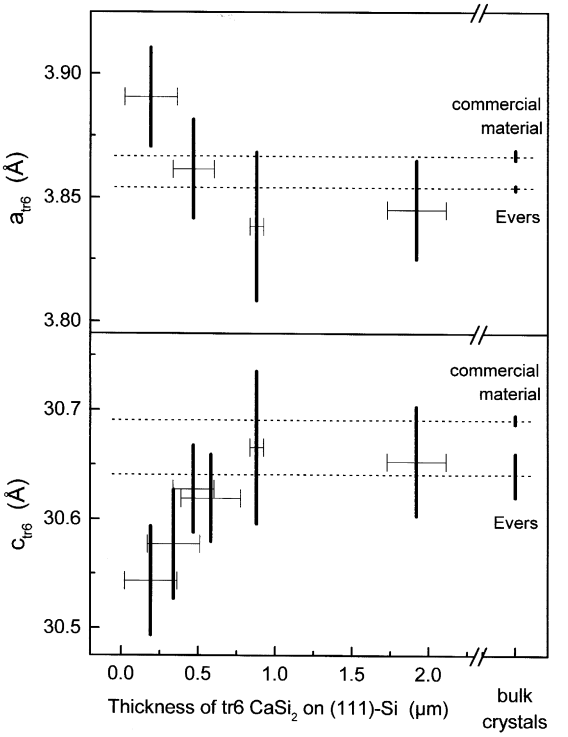


Fig. 6. Comparison of the *a* and *c* lattice constants of the tr6 modification in epitaxial $CaSi_2$ on (1 1 1)-Si as a function of the estimated thickness of the tr6 film. The solid bars indicate the distribution of lattice constants as determined from the full width at half maximum of the diffraction peaks. Included are the data obtained by Evers on $CaSi_2$ single crystals [15] and data obtained on commercial $CaSi_2$ (Chempur).

### 3.2. $CaSi_2$ on (1 1 0)-Si

Although two {1 1 1}-planes perpendicular to and two {1 1 1}-planes with an angle of about 35°

with respect to the surface are present in (1 1 0)-Si substrates, we only find the formation of $CaSi_2$ films with inclined layering. Again, under proper growth conditions, continuous films can be formed as shown in Fig. 7. The obvious fringe pattern in the top view is caused by the grain boundaries and marks the [1 $\bar{1}$ 0] direction of the substrate (see Fig. 2). As expected, the $CaSi_2$/Si interface is not as sharp as in the case of (1 1 1)-substrates. In contrast, using TEM we find a step pattern at the interface, which maximizes the interface area with silicide (0 0.1) layers being parallel to the $\{1\,1\,1\}$ substrate planes. One of these steps is shown in the cross-sectional HRTEM micrograph in Fig. 8. The interface between the (0 0 .1) $CaSi_2$ layers and the (1 1 1)-Si plane is again atomically abrupt, as in the case of growth on (1 1 1)-Si substrates. Between adjacent interfaces of this kind, a second rough type of interface is formed which is parallel to the (1 1 $\bar{1}$)-Si plane indicated in Fig. 8. This second interface has a lattice mismatch of about 2%, ten Si-planes (thickness 31.3 Å) nearly corresponding to one unit cell of tr6 $CaSi_2$ ($c_{tr6}$ = 30.6 Å), which is considerably larger than the mismatch of the (0 0 .1) layer of $CaSi_2$ with a (1 1 1)-Si layer of 0.4%. It is therefore easy to understand why only inclined $CaSi_2$ platelets and no vertical platelets are formed on (1 1 0)-Si substrates.

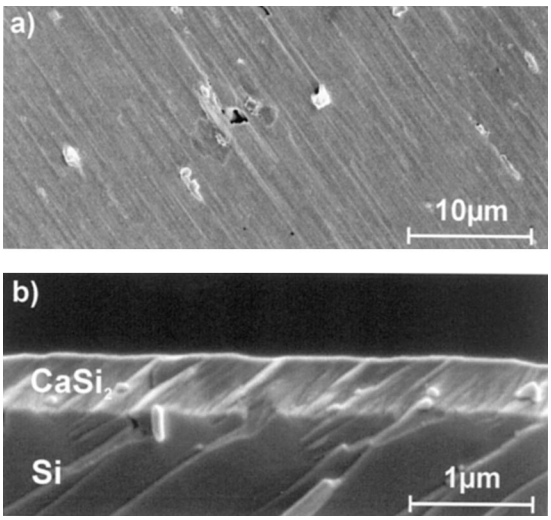


Fig. 7. Top view (a) and side view (b) scanning electron micrographs of epitaxial $CaSi_2$ on (1 1 0)-Si substrates (substrate misorientation $<0.4^\circ$, substrate temperature $\approx 900^\circ$C, Ca flow $\approx 0.2$ μm/min, growth time 20 min).

Despite of the rough interface with Si, the resulting $CaSi_2$ film on (1 1 0)-Si has a crystalline quality comparable to that of the films grown on (1 1 1)-Si. We find linewidths of 0.13° for $2\Theta$ and 0.25° for $\Omega$ scans of the *00.12* reflex of tr6 $CaSi_2$. Fig. 9 shows

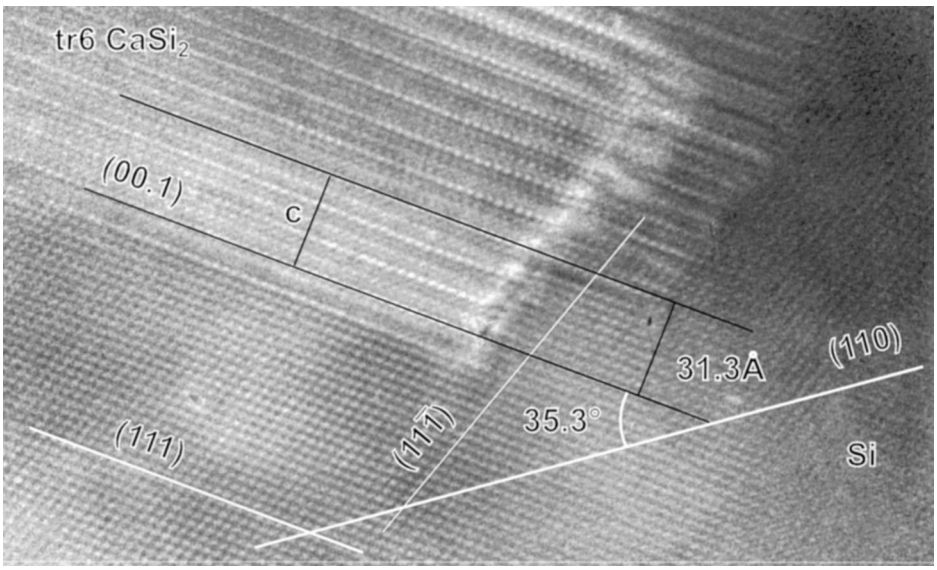


Fig. 8. High-resolution transmission electron micrograph of the $CaSi_2$/Si interface for growth on (1 1 0)-Si substrates.

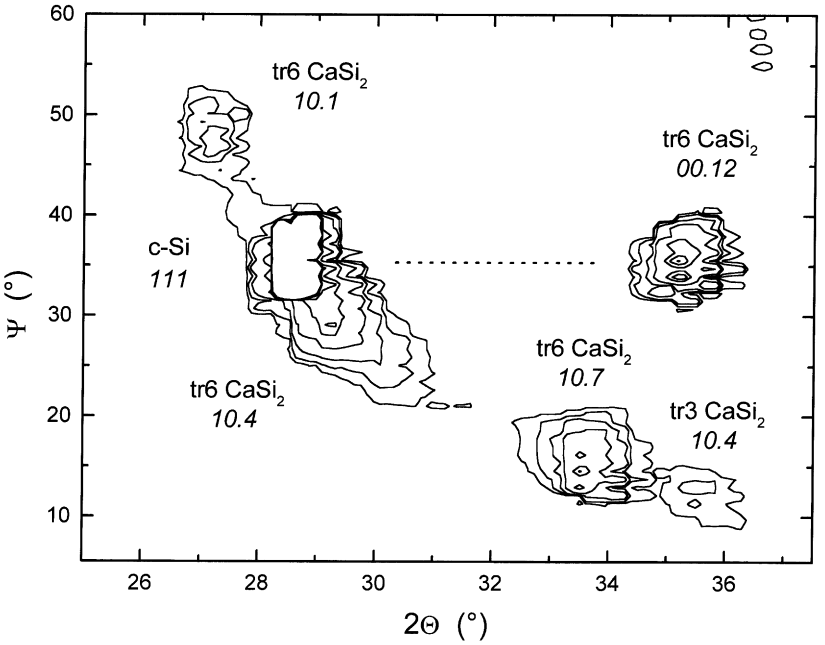


Fig. 9. X-ray diffraction $2\Theta$–$\Psi$-contour map of a 1 μm thick $CaSi_2$ epilayer on (1 1 0)-Si. $\Psi$ is the angle between the (1 1 0) substrate surface and the scattering plane of the respective reflex. The rectangular shape of especially the c-Si *111* reflex is caused by the detector slit width of 0.5°.

a $2\Theta$–$\Psi$-contour map of a typical 1 μm thick $CaSi_2$ layer on (1 1 0)-Si where $\Psi$ is the angle between the substrate surface and the scattering plane of the respective reflex. The symmetric *00.12* reflex of the $CaSi_2$ appears at the same $\Psi$ value as the 1 1 1 Si reflex, as expected for (0 0 .1) $CaSi_2$ layers parallel to the (1 1 1) Si layers. More precise measurements have shown a deviation of 0.5° possibly due to the tensile strain at the step-formed interface. The *10.4* reflex of tr3 $CaSi_2$ is also seen in the contour map, indicating that again both polytypes are formed. Finally, in some cases twins are formed, with the (0 0 .1) $CaSi_2$ layers parallel either to the (1 1 1)- or the (1 1 $\bar{1}$)-Si substrate layers. Preliminary experiments indicate that twin formation can be suppressed by the use of vicinal substrates.

### 3.3. Siloxene on (1 1 1)-Si

Chemical transformation of $CaSi_2$ leads to the sheet polymer siloxene [5]. Although epitaxial siloxene films have been obtained from $CaSi_2$ epilayers on all three substrate orientations shown in Fig. 2, we will concentrate here on the structural details of epitaxial siloxene films on (1 1 1)-Si. Since the relatively strong interlayer bonding caused by the Ca cations is replaced by weak van der Waals bonding between neighboring Si layers of siloxene, the crystalline quality of the epilayer decreases during the topochemical reaction. Fig. 10 shows the symmetric *00.6* reflex of siloxene in an $\Omega$- and a $2\Theta$-scan. The $2\Theta$ line width of about 1° is ten times larger than that of the original $CaSi_2$ layer showing a broader distribution of the *c* lattice constant. This distribution is probably caused by the incorporation of slightly varying amounts of $H_2O$ as intercalated water during the wet chemical reaction. The peak position at 14.25° leads to an interlayer distance of 6.2 Å, in accordance with the range of *c* values reported by other groups [6,16]. On the other hand, the increased line width of 4° for the rocking curve is not surprising considering the ease of distortion in a layered compound with weak interlayer bonding. However, the possibility

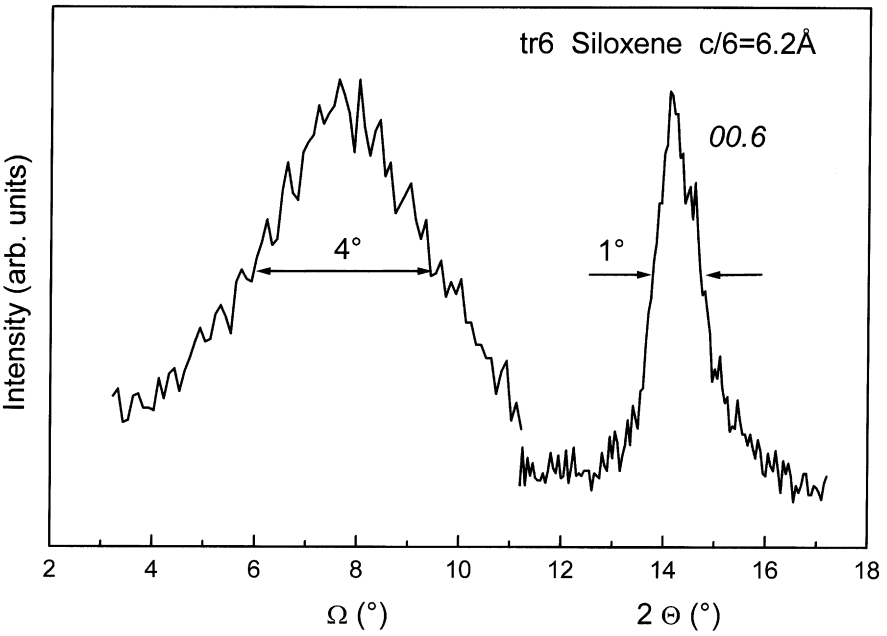


Fig. 10. Comparison of the Bragg–Brentano and rocking curve linewidths of a 0.8 μm thick siloxene epilayer on (1 1 1)-Si. The detector slit width was 0.5°.

to study a sub-μm siloxene layer with its fairly low scattering cross section by XRD shows the surprisingly high crystalline quality of the layer.

Whereas the structure of a single siloxene layer in the meantime has been fairly well established, the exact stacking sequence of the layers and therefore the unit cell of a siloxene crystal is so far unknown. Weiss et al. have observed that, while the stacking sequence in their samples was more or less turbostratic, dislocations of $(n/3)a$ between adjacent layer pairs were favored ($n = 1, 2,...$), corresponding to a stacking with the center of a Si chair directly above a Si atom in the next layer [16]. This registered stacking has later been confirmed by Dahn et al. [17] and Dettlaff-Weglikowska et al. [6]. However, both groups still had to assume a significant amount of random stacking to properly describe their XRD powder data. The weak interlayer bonding as well as in some cases the presence of both tr6 and tr3 $CaSi_2$ polytypes in the starting material makes the determination of the exact stacking sequence from XRD measurements on platelets very difficult. In contrast, the epitaxial siloxene films on (1 1 1)-Si are of sufficient quality to allow such an investigation.

As discussed above, Fig. 1 shows the crystal structure of the tr6 and tr3 modifications of $CaSi_2$ which differ by their stacking sequence or, equivalently, by the rotation of subsequent silicon double-layers. It is very difficult to imagine that the low-temperature topochemical transformation into siloxene will alter that sequence, in particular the orientation of the silicon layers, since this would amount to the displacement of whole double-layers on a large scale or to "umbrella" transformations flipping the constituent chairs of the double-layers. The stacking sequence of siloxene reported so far [16,17] would correspond to a tr3 modification, i.e. with a stacking sequence of the Si sub-lattice corresponding to that in tr3 $CaSi_2$ (dislocations of $(1/3)a$). We have used the pure tr6 $CaSi_2$ films reported above to study the stacking sequence in siloxene selectively obtained from this modification. Fig. 11 shows a $2\Theta$–$\Psi$-map of this sample together with the expected diffraction peak positions for the tr6 and tr3 modifications of siloxene. $\Psi$ is the angle between the (1 1 1) substrate surface and the scattering plane of the respective reflex. The good agreement of the experimentally observed

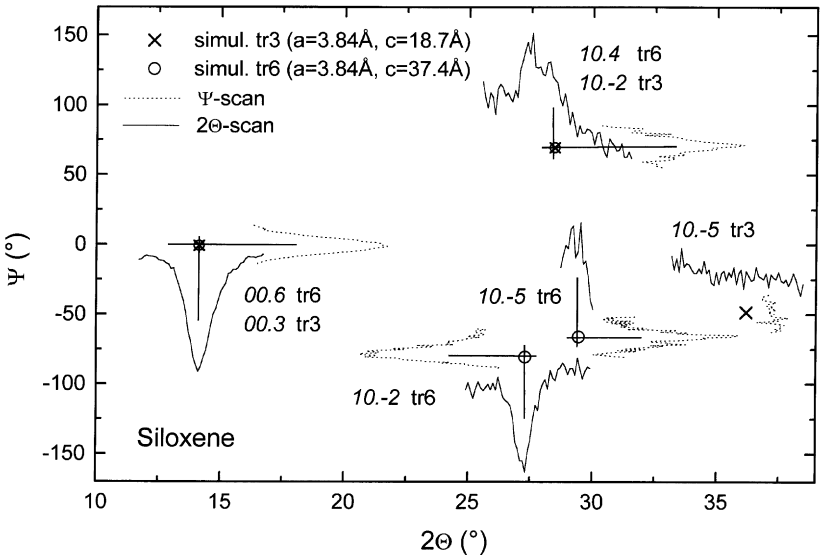


Fig. 11. X-ray diffraction $2\Theta$-$\Psi$-map of a siloxene film on (1 1 1)-Si obtained from a $CaSi_2$ epilayer only consisting of the tr6 modification. $\Psi$ is the angle between the (1 1 1) substrate surface and the scattering plane of the respective reflex. For comparison, the X-ray diffraction peak positions expected for the tr3 and tr6 modifications of siloxene are also given. The peak intensities are normalized and should not be compared. The detector slit width was 2°.

Table 1
Crystallographic details of the tr6-modification of siloxene. Idealized space group P3m1, $a = 3.84$ Å, $c = 37.2$ Å. The positions of the H atoms have not been refined

| | Atom | Site | $x$ | $y$ | $z$ | | | |
|---|---|---|---|---|---|---|---|---|
| 4 | Si | 1a | 0 | 0 | 0.1770 | 0.3440 | 0.6560 | 0.8230 |
| 4 | Si | 1b | 1/3 | 2/3 | 0.0107 | 0.3227 | 0.4897 | 0.8437 |
| 4 | Si | 1c | 2/3 | 1/3 | 0.1563 | 0.5103 | 0.6773 | 0.9893 |
| 2 | O | 1a | 0 | 0 | 0.6130 | 0.7800 | | |
| 2 | O | 1b | 1/3 | 2/3 | 0.2797 | 0.4467 | | |
| 2 | O | 1c | 2/3 | 1/3 | 0.1133 | 0.9463 | | |
| 2 | H | 1a | 0 | 0 | 0.2184 | 0.3851 | | |
| 2 | H | 1b | 1/3 | 2/3 | 0.0517 | 0.8851 | | |
| 2 | H | 1c | 2/3 | 1/3 | 0.5517 | 0.7184 | | |
| 2 | 1/3 H | 3d | 0.8636 | 0.1364 | 0.6017 | 0.7687 | | |
| 2 | 1/3 H | 3d | 0.1970 | 0.8030 | 0.2684 | 0.4354 | | |
| 2 | 1/3 H | 3d | 0.5304 | 0.4696 | 0.1020 | 0.9350 | | |

XRD peaks and the simulation for the tr6 siloxene modification as well as the failure to observe the $10.\bar{5}$ peak characteristic for the tr3 modification prove that siloxene indeed remains in the tr6 polytype when prepared from tr6 $CaSi_2$ only. The small deviation in the $\Psi$-scan of the $10.\bar{2}$ reflex is caused by the nearly glancing incidence ($\Psi$ near 90°) whereas the deviation in $2\Theta$ of the *10.4* reflex is due to the overlying $10.\bar{2}$ reflex. Comparing the intensities of the symmetric *00.6* and the asymmetric $10.\bar{2}$ reflexes with the theoretical intensities allows us to estimate that less than 5% of the siloxene

layers are stacked randomly. This shows that, if the chemical transformation is well controlled, the defined crystal structure of the silicide keeps fully intact. The crystal structure of tr6 siloxene obtained is also shown in Fig. 1, the corresponding atom positions and Wyckoff sites are listed in Table 1. Taking into account only Si and O atoms, siloxene can be described by the space group P3m1 (No. 156) [6]. This symmetry is broken by the presence of the single H atom at the hydroxyl group, which, however, is not observed in XRD. Ab initio calculations have shown that the H atom at the OH group will be pointing towards an H atom of the adjacent layer [18]. We have accordingly added a H atom on one of the three equivalent *d* Wyckoff sites of the space group to complete the structure in Fig. 1 and Table 1. However, the existence of a broad IR absorption band at 3500–3600 $cm^{-1}$ suggests the formation of H-bonds in some parts of the structure, which indicates that the OH-groups also exist in an orientation shifted by 180° to the orientation given above. The exact H-position and the interlayer bonding is subject to further investigations.

## 4. Conclusions

In this paper we have discussed in detail the reactive deposition epitaxy of $CaSi_2$ on Si substrates. It was shown that films with rocking curves widths as low as 0.25° could be grown both on (1 1 1) and (1 1 0)-Si substrates. $CaSi_2$ films preferentially form with their (0 0 .1) planes parallel to a $\{1\ 1\ 1\}$ plane of the silicon substrate. We therefore obtain $CaSi_2$ films with Si double-layers parallel to the substrate surface for (1 1 1)-Si substrates and inclined with an angle of 35° for (1 1 0) substrates. In general, the layers consist of a mixture of the two $CaSi_2$ modifications tr3 and tr6 with the tr6 modification forming directly on the substrate. The $CaSi_2$ films can be topochemically transformed into epitaxial siloxene films, which still have a crystallinity sufficient to study the exact stacking sequence in this material. Most importantly, we have developed a thin film growth technique to prepare Si sheet polymers with different orientations with respect to the substrate. This is a prerequisite to further application of these materials in optoelectronic decives.

## Acknowledgements

The authors acknowledge the financial support of the Deutsche Forschungsgemeinschaft through Schwerpunktprogramm "Silicium-Chemie" (Stu 134/4-2). They are also thankful to J. Evers for providing the unpublished thermal expansion data of $CaSi_2$.

## References

[1] R.T. Tung, in: S. Mahajan (Ed.), Handbook of Semiconductors, Vol. 3, Elsevier, Amsterdam, 1994.
[2] Strukturberichte 1 (1913–1928) 175.
[3] J. Evers, J. Solid State Chem. 28 (1979) 369.
[4] K.H. Janzon, H. Schäfer, A. Weiss, Z. Naturforsch. 23b (1968) 1544.
[5] F. Wöhler, Lieb. Ann. 127 (1863) 257.
[6] U. Dettlaff-Weglikowska, W. Hönle, A. Molassioti-Dohms, S. Finkbeiner, J. Weber, Phys. Rev. B 56 (1997) 13132.
[7] G. Schott, Z. Chemie (Leipzig) 3 (1963) 41.
[8] G. Vogg, N. Zamanzadeh-Hanebuth, M.S. Brandt, M. Stutzmann, M. Albrecht, Chem. Monthly 130 (1999) 79.
[9] J.F. Morar, M. Wittmer, J. Vac. Sci. Technol. A 6 (1988) 1340.
[10] J.F. Morar, M. Wittmer, Phys. Rev. B 37 (1988) 2618.
[11] R. Braungart, H. Sigmund, Z. Naturforsch. 35a (1980) 1268.
[12] M.A. Nicolet, S.S. Lau, in: N.G. Einspruch (Ed.), VLSI Electronics, Vol. 6, Academic Press, New York, 1983.
[13] R.M. Walser, R.W. Bene, Appl. Phys. Lett. 28 (1976) 624.
[14] M.S. Brandt, A. Breitschwerdt, H.D. Fuchs, A. Höpner, M. Rosenbauer, M. Stutzmann, J. Weber, Appl. Phys. A 54 (1992) 567.
[15] J. Evers, private communication.
[16] A. Weiss, G. Beil, H. Meyer, Z. Naturforsch. 35 (1979) 25.
[17] J.R. Dahn, B.M. Way, E. Fuller, Phys. Rev. B 48 (1993) 17872.
[18] C.G. Van de Walle, J.E. Northrup, Phys. Rev. Lett. 70 (1993) 1116.